Supplemental Data

"A Pre-Targeted PET Imaging Strategy Based on Bioorthogonal Diels-Alder Click Chemistry"

Brian M. Zeglis, Kuntal K. Sevak, Thomas Reiner, Priya Mohindra, Sean D. Carlin, Pat Zanzonico, Ralph Weissleder, and Jason S. Lewis

Supplemental Methods.

Instrumentation. All instruments were calibrated and maintained in accordance with standard quality-control procedures. UV-Vis measurements were taken on a Thermo Scientific NanoDrop 2000 Spectrophotometer. NMR spectroscopy was performed on a Bruker 500 MHz NMR with TopSpin 2.1 software for spectrum analysis.

HPLC. HPLC was performed using a Shimadzu HPLC equipped with a C_{18} reversed-phase column (Phenomenex Luna analytical 4.6 x 250 mm), 2 LC-10AT pumps, a SPD-M10AVP photodiode array detector, a Bioscan Flow Counts radioactivity detector, and a gradient of 0:100 MeCN:H_2O (both with 0.1% TFA) to 100:0 MeCN:H_2O over 15 min.

Synthesis of 2,2',2''-(2-(4-(5-((4-(1,2,4,5-tetrazin-3-yl)benzyl)amino)-5-oxopentanamido)benzyl)-1,4,7-triazonane-1,4,7-triyl)triacetic acid (Tz-Bn-NOTA). NH_2-Bn-NOTA (1.25×10^{-2} mmol) was dissolved in 600 μL $NaHCO_3$ buffer (pH 8.1), and 2 μL DIEA was added to this solution. Subsequently, amine-reactive tetrazine (Tz-NHS, 1.25×10^{-3} mmol) was added to this solution, and the resultant solution was stirred at room temperature for 3 h. After the allotted time, the reaction was purified via semi-preparative, reversed-phase C_{18} HPLC to remove unreacted NH_2-Bn-NOTA [0:100 MeCN/H_2O (both with 0.1% TFA) to 100:0 MeCN/H_2O over 30 min, t_R = 9.9 min]. After the removal of solvent, the pink, pure product was obtained in 80% yield (0.7 mg, 1.0×10^{-3} mmol). ^{1}H NMR (500 MHz, DMSO), δ, ppm: 10.59 (s, 1H), 9.87 (s, 1H), 8.5 (m, 4H), 7.55 (dd, 4H), 7.18 (bs, 2H), 4.41 (d, 2H), 3.9-3.5 (m, 4H), 3.1-2.6 (m, 9 H), 2.37 (t, 4H), 2.25 (t, 4H), 1.89 (t, 4H). ESI-MS: 692.6 $[M+H]^+$. UV-Vis: $\varepsilon_{519} = 294\ M^{-1}cm^{-1}$.

Synthesis of ^{64}Cu-NOTA-A33. Freshly prepared and purified ^{64}Cu-Tz-Bn-NOTA was combined with A33-TCO in 500 μL PBS (pH 7.4) such that the molar ratio of Tz:mAb was 4:1, and the resultant solution was incubated at RT for 30 min. After 30 min, the reaction progress was assayed using radio-TLC with an eluent of 50 mM EDTA, pH 5, and the reaction was quenched 50 μL of the same EDTA solution. The ^{64}Cu-NOTA-A33 was then purified using size-exclusion chromatography (Sephadex G-25 M, PD-10 column, GE Healthcare; dead volume = 2.5 mL, eluted with 500 mL fractions of PBS, pH 7.4) and concentrated, if necessary, with centrifugal column filtration. The radiochemical purity of the crude and final radiolabeled bioconjugate was assayed by radio-ITLC. In the radio-TLC experiments, ^{64}Cu-NOTA-A33 remains at the baseline, while $^{64}Cu^{2+}$ ions, free [^{64}Cu]-EDTA, and ^{64}Cu-Tz-Bn-NOTA elute with or close to the solvent front. Crude radiochemical yields of 80-90% were obtained, and post-purification radiochemical purities were >99% (corresponding to specific activities of 3.0-3.5 mCi/mg).

Stability of ^{64}Cu-Tz-Bn-NOTA. ^{64}Cu-Tz-Bn-NOTA was incubated with agitation (550 rpm) at 37 °C in 500 μL of either PBS (pH 7.4) or mouse serum. At each prescribed time-point, 100 μL of the solution was removed and placed into a 1.7 mL microcentrifuge tube. For the PBS samples,

the compound was injected directly onto the HPLC. For the serum samples, 100 μL cold MeCN was added to the serum, and the resultant mixture was vortexed and centrifuged at 14,000 rpm for 5 min. After this, the clear supernatant was removed, moved to a new 1.7 mL microcentrifuge tube, and centrifuged again at 14,000 rpm for 5 min. The clear supernatant from this second spin was then injected into the HPLC. The residual protein from the centrifuge spins was checked for radioactivity, and only minimal residual activity remained (<1% of the starting ^{64}Cu). The fraction of intact ^{64}Cu-Tz-Bn-NOTA was determined by integrating the peak corresponding to the compound and dividing by the integral over the whole HPLC run [0:100 MeCN/H_2O (both with 0.1% TFA) to 100:0 MeCN/H_2O over 30 min, t_R = 9.9 min]. Both the injection loop and column were monitored to detect the presence of residual activity trapped in these locations.

***In Vivo* Stability Measurements of ^{64}Cu-Tz-Bn-NOTA.** Healthy athymic nude mice were injected via tail vein with ^{64}Cu-Tz-Bn-NOTA (100 μCi in 200 μL 0.9% sterile saline). After 15 min, 30 min, 60 min, 120 min, 6 h, and 12 h, the mice were euthanized via $CO_{2(g)}$ asphyxiation, and the blood was removed via cardiac puncture. The blood was placed in heparin-coated centrifuge tubes, weighed, and counted for activity on a gamma counter. Subsequently, the blood was centrifuged to separate the serum. Subsequently,100 μL cold MeCN was added to the serum, and the resultant mixture was vortexed and centrifuged at 14,000 rpm for 5 min. After this, the clear supernatant was removed, moved to a new 1.7 mL microcentrifuge tube, and centrifuged again at 14,000 rpm for 5 min. The clear supernatant from this second spin was then injected into the HPLC. The residual protein from the centrifuge spins was checked for radioactivity, and only minimal residual activity remained (<2% of the starting ^{64}Cu). The fraction of intact ^{64}Cu-Tz-Bn-NOTA was determined by integrating the peak corresponding to the compound and dividing by the integral over the whole HPLC run [0:100 MeCN/H_2O (both with 0.1% TFA) to 100:0 MeCN/H_2O over 30 min, t_R = 9.9 min]. Both the injection loop and column were monitored to detect the presence of residual activity trapped in these locations.

Measuring the Yield of the Tz-TCO Ligation. To a 1 μM solution of A33-TCO in PBS (pH 7.4 100 μL) or mouse serum (100 μL), an appropriate amount of ^{64}Cu-Tz-Bn-NOTA was added to create final ^{64}Cu-Tz-Bn-NOTA:mAb ratios of 1:5, 1:1, and 5:1. The resultant solutions were incubated at 37 °C for 30 min with agitation (550 rpm). After the prescribed amount of time, the yield of the reaction was assayed using radio-TLC with an eluent of 50 mM EDTA, pH 5. In the radio-TLC experiments, the resultant ^{64}Cu-NOTA-A33 remains at the baseline, while ^{64}Cu-Tz-Bn-NOTA elutes with or close to the solvent front. The yield was calculated by dividing the integral of the ^{64}Cu-NOTA-A33 peak over the integral of the entire chromatograph.

Determining the Effect of Prolonged 37 °C Incubation on the Tz-TCO Ligation. To determine the effect of prolonged incubation at 37 °C on the click ligation, A33-TCO (1 μM) was incubated at 37 °C with agitation (550 rpm) in PBS (pH 7.4, 100 μL) or mouse serum (100 μL) for 2 d. After the allotted time, ^{64}Cu-Tz-Bn-NOTA was added to create final ^{64}Cu-Tz-Bn-NOTA:mAb ratios of 1:5 or 1:1, and the resultant solutions were further incubated at 37 °C for 30 min with agitation (550 rpm). To determine the extent of the click reaction, the same protocol was employed as is described above in "Measuring the Yield of the Click Ligation".

Modification of A33 with DFO-NCS. A33 (2 mg, 13.3 nmol) was dissolved in 1 mL of phosphate buffered saline (pH 7.4), and the pH of the solution was adjusted to 8.8-9.0 with $NaHCO_3$ (0.1 M). To this solution was added an appropriate volume of SCN-DFO in DMSO (5-10 mg/mL) to yield a chelator:mAb reaction stoichiometry of 5:1. The resultant solution was incubated with gentle shaking for 30 min at 37 ºC. After 30 min, the modified antibody was purified using centrifugal filter units with a 50,000 molecular weight cut off (Amicon™ Ultra 4

Centrifugal Filtration Units, Millipore Corp., Billerica, MA) and phosphate buffered saline (PBS, pH 7.4).

Radiolabeling of A33-DFO with ^{89}Zr. A33-DFO (0.2-0.3 mg) was added to 200 μL buffer (PBS, pH 7.4). [^{89}Zr]Zr-oxalate (29.6-37 MBq, 800-1000 μCi) in 1.0 M oxalic acid was adjusted to pH 7.2-8.5 with 1.0 M Na_2CO_3. After evolution of CO_2(g) stops, the ^{89}Zr solution was added to the antibody solution, and the resultant mixture was incubated at room temperature for 1 h. After 1 h, the reaction progress was assayed using radio-TLC with an eluent of 50 mM EDTA, pH 5, and the reaction was quenched 50 μL of the same EDTA solution. The ^{89}Zr-DFO-A33 was purified using size-exclusion chromatography (Sephadex G-25 M, PD-10 column, GE Healthcare; dead volume = 2.5 mL, eluted with 500 mL fractions of PBS, pH 7.4) and concentrated, if necessary, with centrifugal filtration. The radiochemical purity of the crude and final radiolabeled bioconjugate was assayed by radio-ITLC. In the ITLC experiments, ^{89}Zr-DFO-A33 remains at the baseline, while $^{89}Zr^{4+}$ ions and [^{89}Zr]-EDTA elute with the solvent front. Crude radiochemical yields of 80-90% were obtained, and post-purification radiochemical purities were >99% (corresponding to specific activities of 3.5-4.5 mCi/mg).

Chelate Number. The number of accessible DFO or NOTA chelates conjugated to the antibodies was measured by radiometric isotopic dilution assays following methods similar to those described by Anderson, *et al*. and Holland, *et al*.(1, 2) All experiments were performed in triplicate.

Radiolabeled Antibody Stability Assays. The stability of the ^{89}Zr-DFO-A33 and ^{64}Cu-NOTA-A33 bioconjugates with respect to radiochemical purity and loss of radioactivity from the antibody was investigated *in vitro* by incubation of the antibodies in mouse serum for 48 h (^{64}Cu) or 7 (^{89}Zr) days at room temperature of 37 °C (n = 3 for all measurements). The radiochemical purity of the antibodies was determined via radio-TLC with an eluent of 50 mM EDTA pH 5.0.

Immunoreactivity Assays. The immunoreactivity of the ^{89}Zr-DFO-A33 and ^{64}Cu-NOTA-A33 bioconjugates was determined using specific radioactive cellular-binding assays following procedures derived from Lindmo, *et al.(3, 4)* To this end, SW1222 cells were suspended in microcentrifuge tubes at concentrations of 5.0, 4.0, 3.0, 2.5, 2.0, 1.5, and 1.0 x 10 ^{6} cells/mL in 500 μL PBS (pH 7.4). Aliquots of either ^{89}Zr-DFO-A33 or ^{64}Cu-NOTA-A33 (50 μL of a stock solution of 10 μCi in 10 mL of 1% bovine serum albumin in PBS pH 7.4) were added to each tube (n = 4; final volume: 550 μL), and the samples were incubated on an mixer for 60 minutes at room temperature. The treated cells were then pelletted via centrifugation (3000 rpm for 5 minutes), re-suspended, and washed twice with cold PBS before removing the supernatant and counting the activity associated with the cell pellet. Self-blocking experiments with radiolabeled antibody of extremely low specific activity (*i.e.*, 1000-fold excess of unlabeled antibody) were performed as a negative control. The activity data were background-corrected and compared with the total number of counts in appropriate control samples. Immunoreactive fractions were determined by linear regression analysis of a plot of (total/bound) activity against (1/[normalized cell concentration]). No weighting was applied to the data, and data was obtained in triplicate. As a negative control, immunoreactivity assays were performed in which a 250-fold excess of cold NOTA-A33 was added to the [^{64}Cu]-NOTA-A33 formulation, and these revealed an immunoreactivity of 1.6 ± 1.1%.

Cell Culture. Human colorectal cell line SW1222 was obtained from the Ludwig Institute of Cancer Research and maintained in Minimum Essential Medium, supplemented with 10% heat-inactivated fetal calf serum, 2.0 mM glutamine, 100 units/mL penicillin, and 100 units/mL

streptomycin in a 37°C environment containing 5% CO_2. Cell lines were harvested and passaged weekly using a formulation 0.25% trypsin/0.53 mM EDTA in Hank's Buffered Salt Solution without calcium and magnesium.

Xenograft Models. All experiments we performed under an Institutional Animal Care and Use Committee-approved protocol, and the experiments followed institutional guidelines for the proper and humane use of animals in research. Six-eight week-old athymic nude female (Hsd: Athymic Nude-nu) mice were obtained from Harlan Laboratories (Indianapolis, IN). Animals were housed in ventilated cages, were given food and water *ad libitum*, and were allowed to acclimatize for approximately 1 week prior to inoculation. SW1222 tumors were induced on the right shoulder by a subcutaneous injection of 5.0 x 10^6 cells in a 200 μL cell suspension of a 1:1 mixture of fresh media : BD Matrigel (BD Biosciences, Bedford, Ma). The xenografts reached ideal size for imaging and biodistribution (~100-150 mm^3) in approximately 9-12 d.

PET Imaging with Labeled Antibodies. PET imaging experiments were conducted on either a microPET Focus rodent scanner (Concorde Microsystems).(5) Mice bearing subcutaneous SW1222 (right shoulder) xenografts (100-150 mm^3, 9-12 days post-inoculation) were administered ^{89}Zr-DFO-A33 (10.2 – 12.0 MBq [275-325 μCi] in 200 μL 0.9% sterile saline) or ^{64}Cu-NOTA-A33 (10.2 – 12.0 MBq [275-325 μCi] in 200 μL 0.9% sterile saline) via intravenous tail vein injection (t = 0). Approximately 5 minutes prior to the PET images, mice were anesthetized by inhalation of 2% isoflurane (Baxter Healthcare, Deerfield, IL)/oxygen gas mixture and placed on the scanner bed; anesthesia was maintained using 1% isoflurane/gas mixture. PET data for each mouse were recorded via static scans at various time points between 6 and 120 h. A minimum of 20 million coincident events were recorded for each scan, which lasted between 10-45 min. An energy window of 350-700 keV and a coincidence timing window of 6 ns were used. Data were sorted into 2-dimensional histograms by Fourier re-binning, and transverse images were reconstructed by filtered back-projection (FBP) into a 128 × 128 × 63 (0.72 × 0.72 × 1.3 mm) matrix. The image data were normalized to correct for non-uniformity of response of the PET, dead-time count losses, positron branching ratio, and physical decay to the time of injection but no attenuation, scatter, or partial-volume averaging correction was applied. The counting rates in the reconstructed images were converted to activity concentrations (percentage injected dose [%ID] per gram of tissue) by use of a system calibration factor derived from the imaging of a mouse-sized water-equivalent phantom containing ^{64}Cu or ^{89}Zr. Images were analyzed using ASIPro VM™ software (Concorde Microsystems).

Acute Biodistribution with Labeled Antibodies. Acute *in vivo* biodistribution studies were performed in order to evaluate the uptake of ^{89}Zr-DFO-A33 and ^{64}Cu-NOTA-A33 in mice bearing subcutaneous SW1222 (right shoulder) xenografts (100-150 mm^3, 9-12 days post-inoculation). Tumor-bearing mice were randomized before the study and were warmed gently with a heat lamp for 5 min before administration of ^{89}Zr-DFO-A33 (0.55 – 0.75 MBq [15-20 μCi] in 200 μL 0.9% sterile saline, 4-6 μg) or ^{64}Cu-NOTA-A33 (0.55 – 0.75 MBq [15-20 μCi] in 200 μL 0.9% sterile saline, either 4-6 μg or 100 μg) via intravenous tail vein injection (t = 0). Animals (n = 4 per group) were euthanized by CO_2(g) asphyxiation at 4, 24, 48, 72, 96, and 120 h (^{89}Zr) or 4, 12, 24, and 48 h (^{64}Cu). After asphyxiation, 13 tissues (including tumor) were removed, rinsed in water, dried in air for 5 min, weighed, and counted in a gamma counter calibrated for either ^{64}Cu or ^{89}Zr. Counts were converted into activity using a calibration curve generated from known standards. Count data were background- and decay-corrected to the time of injection, and the percent injected dose per gram (%ID/g) for each tissue sample was calculated by normalization to the total activity injected. For all biodistribution experiments, stomach, small intestine, and large intestine contents were removed prior to weighing and activity measurements.

Importantly, for the ^{64}Cu-NOTA-A33 biodistribution experiments, experiments were also performed in which the mice received a mass of antibody (100 μg) identical to that administered during the pretargeting experiments, and this alteration affected the *in vivo* profile of the antibody very little either qualitatively and quantitatively.

Labeling A33-TCO with AlexaFluor 680 (AF680). The amine-reactive fluorophore Alexa Fluor680-NHS was obtained from Life Technologies (Carlsbad, CA). A solution of A33-TCO (1.5 mg) was prepared in 1 mL of PBS (pH 7.4). The pH of the resultant solution was adjusted to 8.5-8.7 with 0.1 M $NaHCO_3$. At this point, an appropriate amount of AlexaFluor 680 (10 mg/mL in DMSO) such that the ratio of fluorophore:mAb was 3:1, and the reaction mixture was incubated for 1 h at room temperature with agitation (550 rpm). The consequent A33-TCO-AF680 was purified using size-exclusion chromatography (Sephadex G-25 M, PD-10 column, GE Healthcare; dead volume = 2.5 mL, eluted with 500 mL fractions of PBS, pH 7.4) and concentrated, if necessary, with centrifugal column filtration. Degree of labeling was determined via UV-Vis: absorbance measurements were taken at 280 nm and 680 nm for three separate antibody concentrations. DOL was calculated using the following formulas:

$$A_{mAb} = A_{280} - A_{max}(CF)$$

$$DOL = [A_{max} * MW_{mAb}]/[[mAb] * \varepsilon_{AF680}]$$

where the correction factor (CF) for AF680 was given as 0.05 by the supplier, $MW_{A33} = 150{,}000$, $\varepsilon_{AF680} = 184{,}000$, and $\varepsilon_{280,\,mAb} = 225{,}000$.

Multimodality Fluorescence and PET Imaging. Fluorescence imaging was performed on a Maestro II Fluorescence Imaging System [CRi, Woburn, MA]. Five days prior to imaging, animals were placed on a low auto-fluorescence diet (AIN-76, Harlan Laboratories, Indianapolis, IN). Mice (n = 4) bearing 9-12 day old SW1222 xenografts on the right shoulder were injected via tail vein with 100 μg A33-TCO-AF680. The animals imaged immediately prior to injection of the bioconjugate and at 24 h post-injection. Immediately after this second imaging time point, the animals were injected via tail vein with 250-300 μCi ^{64}Cu-Tz-Bn-NOTA. At 12 h post-injection of the radiotracer (and thus 36 h post-injection of the antibody), the mice were imaged with PET and subsequently imaged a third time for fluorescence. In all cases, the animals were induced at 4% isoflurane/oxygen and maintained at 2% during imaging. Spectral fluorescence imaging was performed using the yellow excitation [615-665 nm] and emission [700 nm, long pass] filter set using 10 nm wavelength steps. Deconvolution of conjugated AlexaFluor680 signal and background autofluorescence was performed in the Maestro II software suite. To avoid signal saturation, the automated exposure time feature was employed.

***Ex Vivo* Tumor and Muscle Imaging.** After the multimodality experiments employing fluorescence and PET imaging, all mice were euthanized, and their SW1222 xenografts and muscle were removed for autoradiography and histology (see below). In two cases, prior to freezing the tissue samples, *ex vivo* fluorescence and PET imaging were performed of the tumor and muscle side-by-side. For details on specific fluorescence and PET imaging procedures, see above.

***Ex Vivo* Autoradiography and Fluorescence Microscopy** Following final imaging, tumors were excised, snap-frozen and embedded in OCT. Series of sequential 10mm thick cryosections were cut and immediately exposed to a phosphor plate for determination of ^{64}Cu distribution.

Digital autoradiographic images at 50 μm pixel size were obtained as previously described.(6) Following autoradiography, sections were fixed in 4% paraformaldehyde and mounted in Vecta-shield mounting medium containing 1.5 mg/ml DAPI. AlexaFluor 680 and DAPI images were acquired at high magnification (×100) using an Zeiss Axioplan2 fluorescence microscope connected to a CCD camera, equipped with a motorized stage (Prior Scientific Instruments, Cambridge, UK, USA) and MetaMorph software (Molecular Devices, Sunnyvale, CA) allowing the individual captured image frames to be rendered into a montage of the entire tumor section. Finally, hematoxylin and eosin staining was performed to visualize tumor morphology, and images acquired in a similar manner Montage images of each stain, all acquired from the same tumor section, were manually registered using Photoshop CS5 software (Adobe Systems). Image rebinning and pixel-by-pixel correlations were carried out as previously described.(7)

Dosimetry. Mouse biodistribution data were expressed as normal-organ mean standard uptake values (SUVs) versus time post-administration. Assuming, in first order, that SUVs are independent of body mass and thus the same among species, the mean SUV in mouse organ i, $SUV_{Organ\ i|Mouse}$, was converted to the fraction of the injected dose in each human organ I, $FID_{Organ\ I|Human}$, using the following formula:

$$FID_{Organ\ i|Human} = SUV_{ran\ i|Mouse} \bullet \frac{\text{Mass of Human Organ i}}{\text{Mass of Human Total Body}}$$

and the organ and total-body masses of the 70-kg Standard Man anatomic model.(8)

These data (corrected for radioactive decay to the time of injection) were then fit to a mono-exponential or bi-exponential time-activity function, depending on the organ. The cumulated activity, or residence time, in human organ i, τ_i, in μCi-h/μCi, was then calculated by analytically integrating the time-activity function in organ i, replacing the biological clearance constant, (λ_{bj}. for each component j of the fitted exponential function with the corresponding effective clearance constant, (λ_{ej} = (λ_{bj} + λ_p, where λ_p is the physical decay constant of the radionuclide.

The resulting organ residence times were entered into the OLINDA computer program to yields the mean organ absorbed doses and effective dose in rad/mCi and rem/mCi, respectively.(9)

Statistical Analysis. Data were analyzed by the unpaired, two-tailed Student's t-test. Differences at the 95% confidence level ($P < 0.05$) were considered to be statistically significant

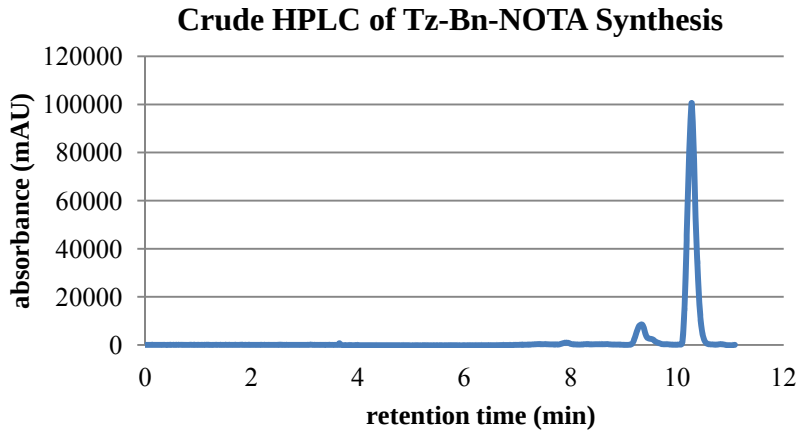

Supplemental Figure 1. Crude HPLC of Tz-Bn-NOTA synthesis to illustrate difference in retention time between the hydrolysis product of Tz-NHS (t_R = 9.3 min) of Tz-Bn-NOTA (t_R = 10.1 min). Monitoring wavelength = 519 nm.

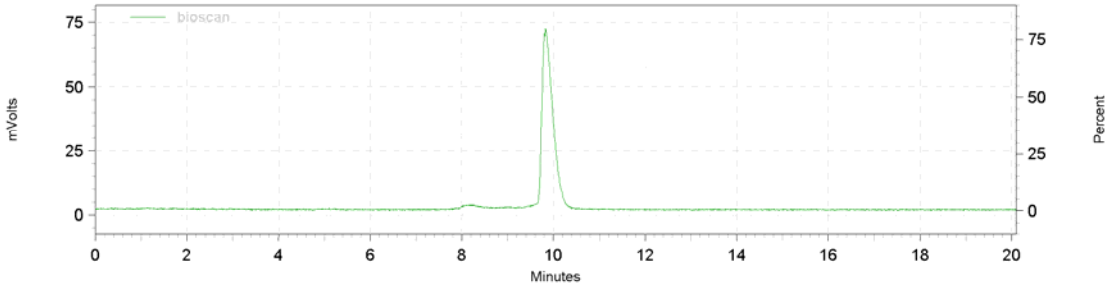

Supplemental Figure 2. Radio-HPLC trace of purified ^{64}Cu-Tz-Bn-NOTA.

	Conditions	
Time	*PBS (pH 7.4)*	*Mouse Serum*
30 min	99.2 ± 1.1	96.6 ± 0.6
1 h	95.6 ± 2.3	93.0 ± 2.5
2 h	91.6 ± 1.9	85.4 ± 6.6
6 h	83.0 ± 2.9	69.0 ± 4.9
12 h	82.1 ± 4.9	31.6 ± 6.1

Supplemental Table 1. Stability of ^{64}Cu-Tz-Bn-NOTA in PBS (pH 7.4) or mouse serum at 37 ºC. The fraction of intact ^{64}Cu-Tz-Bn-NOTA was determined by integrating the peak corresponding to the compound and dividing by the integral over the whole HPLC run [0:100 MeCN/H_2O (both with 0.1% TFA) to 100:0 MeCN/H_2O over 30 min, t_R = 9.9 min]. Both the injection loop and column were monitored to detect the presence of any residual activity trapped in these locations. It is known that tetrazines of this type are unstable, particularly under alkaline conditions; while the serum in this study was of neutral pH, the additional presence of potentially nucleophilic sulfhydryl and amino groups in the serum may accelerate decomposition even at a neutral pH. Nevertheless, given that the rapidity of the cycloaddition reaction with TCO and the rapid pharmacokinetics of the radioligand, it was deemed unlikely that poor serum stability at later time points would be a detriment to the system.

	Conditions	
Tz:mAb Ratio	*PBS (pH 7.4)*	*Mouse Serum*
1:5	91.2 ± 0.9	89.6 ± 1.8
1:1	89.6 ± 0.3	83.0 ± 0.9
5:1	76.7 ± 2.8	75.6 ± 1.0

Supplemental Table 2. Yield of the A33-TCO ligation with ^{64}Cu-Tz-Bn-NOTA in PBS (pH 7.4) and mouse serum. Yields from reactions with varying Tz:mAb stoichiometries were obtained. After incubation for 30 min, the yield of the reaction was assayed using radio-TLC with an eluent of 50 mM EDTA, pH 5. In the radio-TLC experiments, the resultant ^{64}Cu-NOTA-A33 remains at the baseline, while ^{64}Cu-Tz-Bn-NOTA elutes with or close to the solvent front. The yield was calculated by dividing the integral of the ^{64}Cu-NOTA-A33 peak over the integral of the entire chromatograph.

	Conditions	
Tz:mAb Ratio	*PBS (pH 7.4)*	*Mouse Serum*
1:5	90.3 ± 1.0	84.4 ± 2.9
1:1	90.2 ± 1.0	87.0 ± 3.2
5:1	74.2 ± 1.8	73.1 ± 4.2

Supplemental Table 3. The effect of prolonged 37 °C incubation on the click ligation. To determine the effect of prolonged incubation at 37 °C on the click ligation, A33-TCO (1 μM) was incubated at 37 °C with agitation (550 rpm) in PBS (pH 7.4, 100 μL) or mouse serum (100 μL) for 2 d. After the allotted time, ^{64}Cu-Tz-Bn-NOTA was added to create final ^{64}Cu-Tz-Bn-NOTA:mAb ratios of 1:5, 1:1, and 5:1, and the resultant solutions were further incubated at 37 °C for 30 min with agitation (550 rpm). The extent of the reaction was determined with radio-TLC as described elsewhere.

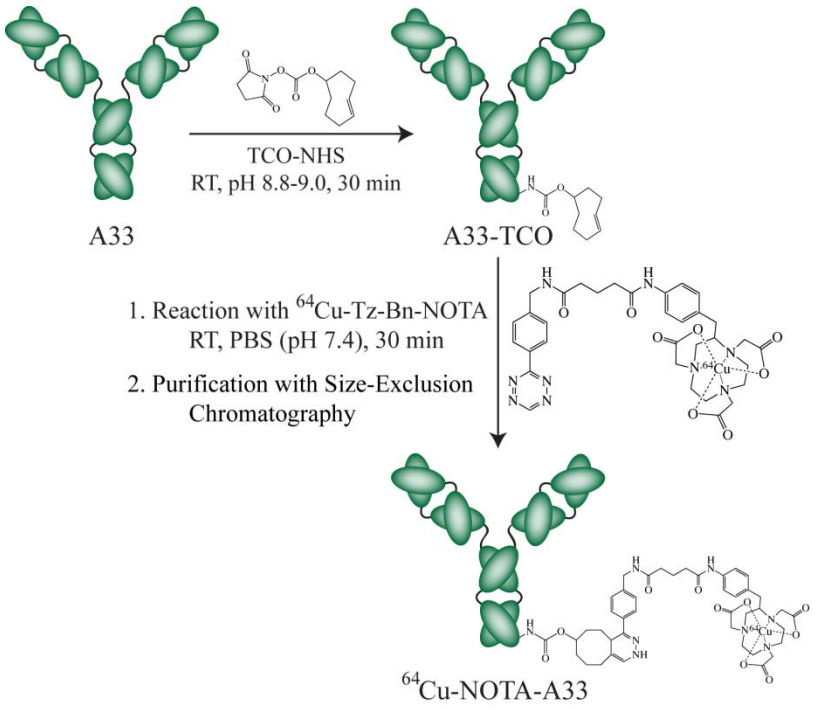

Supplemental Figure 3. Schematic of the click-based synthesis of ^{64}Cu-NOTA-A33.

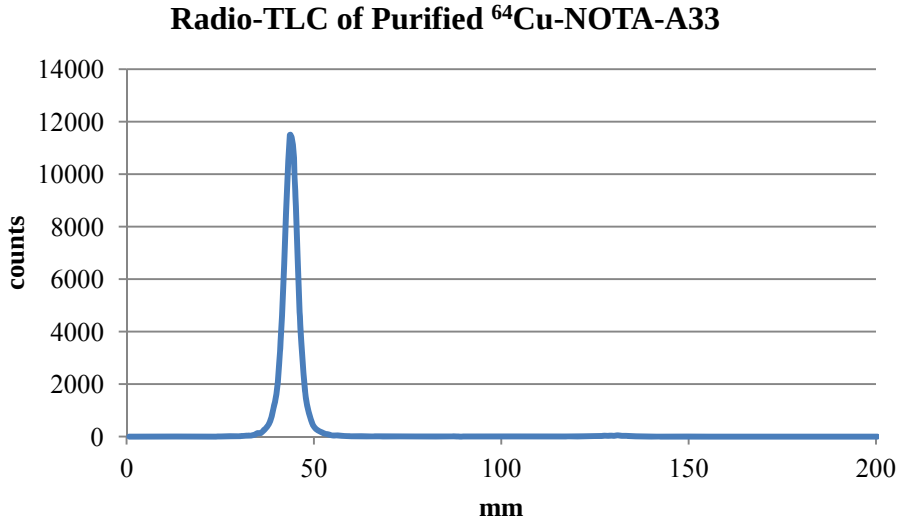

Supplemental Figure 4. Radio-TLC of purified ^{64}Cu-NOTA-A33.

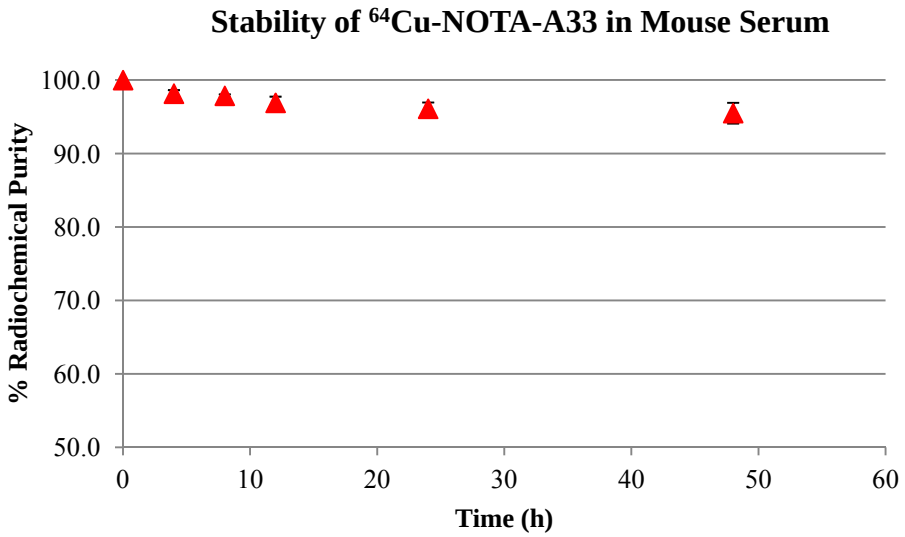

Supplemental Figure 5. Stability of ^{64}Cu-NOTA-A33 to demetalation in mouse serum over the course of 48 h at 37 ºC (red). After 48 h, the construct remained 95.6 ± 1.4% intact. Error bars mark standard deviation from the mean (n = 3).

Time	Activity in Blood (%ID/g)
15 min	3.9 ± 0.7
30 min	2.7 ± 0.3
60 min	2.4 ± 0.3
2 h	1.2 ± 0.4
6 h	1.5 ± 0.3
12 h	0.9 ± 0.4

Supplemental Table 4. The *in vivo* blood residence time of ^{64}Cu-Tz-Bn-NOTA in healthy athymic nude mice (n = 4).

	1 h	4 h	12 h	24 h
Tumor/Blood	1.2 ± 0.2	1.6 ± 0.5	1.8 ± 0.5	1.9 ± 0.6
Tumor/Tumor	1.0 ± 0.1	1.0 ± 0.2	1.0 ± 0.3	1.0 ± 0.3
Tumor/Heart	3.7 ± 0.7	4.5 ± 1.5	4.6 ± 1.2	4.8 ± 1.7
Tumor/Lung	2.6 ± 0.8	2.6 ± 0.7	3.9 ± 1.6	3.8 ± 1.4
Tumor/Liver	1.9 ± 0.2	3.2 ± 0.9	4.5 ± 1.5	3.7 ± 1.0
Tumor/Spleen	6.5 ± 0.8	8.0 ± 3.6	7.1 ± 3.3	8.8 ± 3.0
Tumor/Stomach	9.0 ± 1.7	16.2 ± 8.2	8.1 ± 10.1	24.3 ± 6.9
Tumor/LI	7.8 ± 0.5	1.3 ± 0.5	1.8 ± 0.9	3.4 ± 1.4
Tumor/Feces	0.3 ± 0.1	0.5 ± 0.2	1.6 ± 0.3	2.8 ± 1.2
Tumor/SI	119.5 ± 148.8	10.8 ± 2.8	5.5 ± 3.8	11.4 ± 2.9
Tumor/Kidney	3.1 ± 0.4	4.3 ± 1.6	4.6 ± 1.7	5.6 ± 2.0
Tumor/Muscle	18.4 ± 3.7	29.4 ± 8.5	26.6 ± 6.6	27.0 ± 7.4
Tumor/Bone	13.7 ± 7.6	15.0 ± 13.2	12.0 ± 4.5	13.4 ± 4.5
Tumor/Skin	12.1 ± 2.2	12.6 ± 3.4	10.2 ± 2.8	7.6 ± 3.5

Supplemental Table 5. Tumor to tissue activity ratios from biodistribution data of pre-targeting with A33-TCO and ^{64}Cu-Tz-Bn-NOTA versus time (see *Main Text, Table 1*) in mice bearing subcutaneous SW1222 xenografts (n = 4 for each time point).

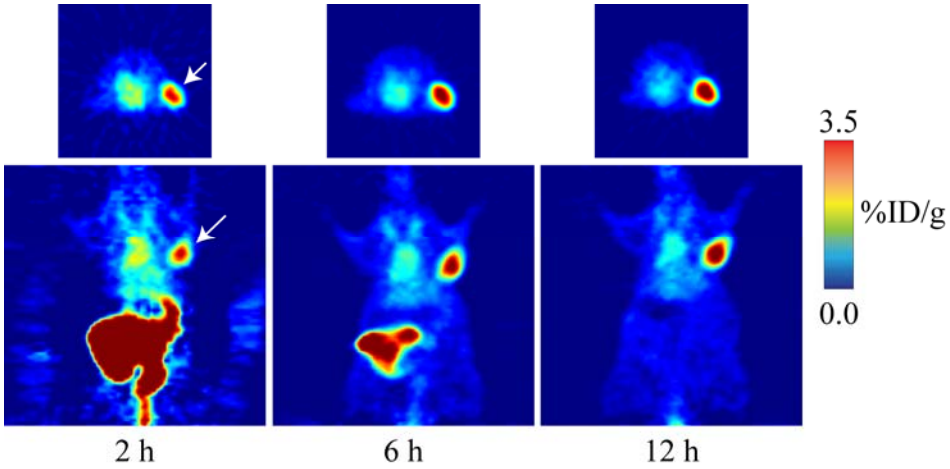

Supplemental Figure 6. PET images of ^{64}Cu-Tz-Bn-NOTA/A33-TCO pre-targeting strategy. Mice bearing subcutaneous SW1222 (right shoulder, white arrow) xenografts (100-150 mm^3, 9-12 days post-inoculation) were administered A33-TCO (100 μg in 200 μL 0.9% sterile saline) via intravenous tail vein injection. After 24 h, the same mice were administered ^{64}Cu-Tz-Bn-NOTA (10.2 – 12.0 MBq, 275-325 μCi, ~1 μg) in 200 μL 0.9% sterile saline via intravenous tail vein injection. The transverse (top) and coronal (bottom) planar images intersect the center of the tumors.

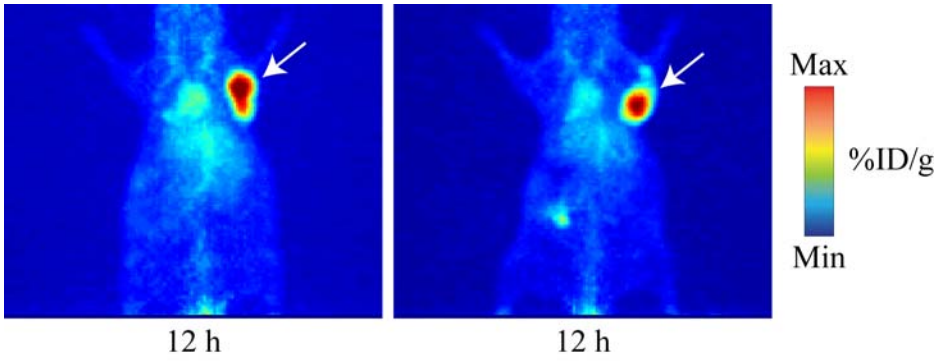

Supplemental Figure 7. Maximum intensity projections at 12 h of ^{64}Cu-Tz-Bn-NOTA/A33-TCO pre-targeting strategy (two different mice). Mice bearing subcutaneous SW1222 (right shoulder, white arrow) xenografts (100-150 mm^3, 9-12 days post-inoculation) were administered A33-TCO (100 μg in 200 μL 0.9% sterile saline) via intravenous tail vein injection. After 24 h, the same mice were administered ^{64}Cu-Tz-Bn-NOTA (10.2 – 12.0 MBq, 275-325 μCi, ~1 μg) in 200 μL 0.9% sterile saline via intravenous tail vein injection.

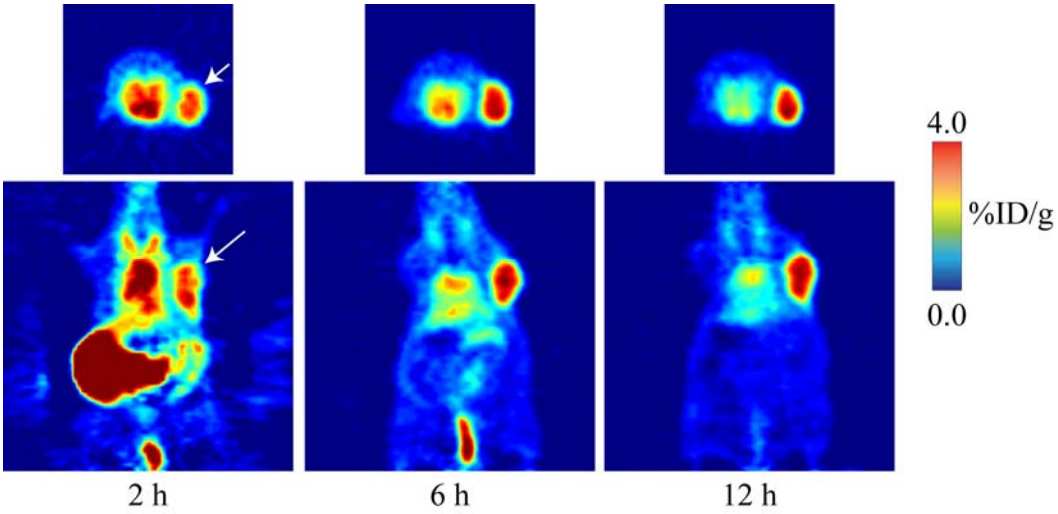

Supplemental Figure 8. Pre-targeting PET imaging. Mice bearing subcutaneous SW1222 (right shoulder, white arrow) xenografts (100-150 mm^3, 9-12 days post-inoculation) were administered A33-TCO (300 μg in 200 μL 0.9% sterile saline) via intravenous tail vein injection. After 24 h, the same mice were administered ^{64}Cu-Tz-Bn-NOTA (10.2 – 12.0 MBq, 275-325 μCi, ~1 μg) in 200 μL 0.9% sterile saline via intravenous tail vein injection. The transverse (top) and coronal (bottom) planar images intersect the center of the tumors.

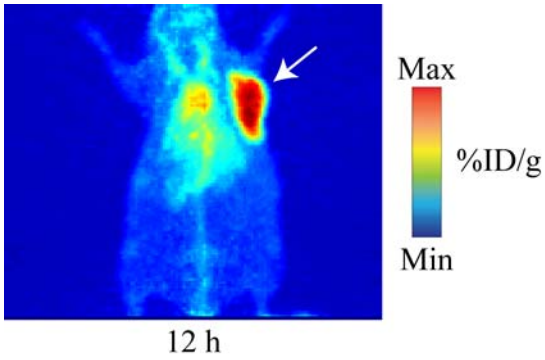

Supplemental Figure 9. Maximum intensity projection at 12 h of pre-targeted PET experiment. PET imaging. Mice bearing subcutaneous SW1222 (right shoulder, white arrow) xenografts (100-150 mm^3, 9-12 days post-inoculation) were administered A33-TCO (300 μg in 200 μL 0.9% sterile saline) via intravenous tail vein injection. After 24 h, the same mice were administered ^{64}Cu-Tz-Bn-NOTA (10.2 – 12.0 MBq, 275-325 μCi, ~1 μg) in 200 μL 0.9% sterile saline via intravenous tail vein injection.

	1 h	4 h	12 h	24 h
Blood	6.2 ± 2.2	5.9 ± 0.9	4.1 ± 0.8	3.5 ± 0.9
Tumor	3.0 ± 0.9	3.7 ± 0.4	3.6 ± 0.2	3.7 ± 1.6
Heart	2.1 ± 0.5	2.0 ± 0.5	1.7 ± 0.4	1.5 ± 0.4
Lung	2.8 ± 0.7	2.2 ± 0.5	1.7 ± 0.1	1.8 ± 0.7
Liver	2.5 ± 1.0	2.2 ± 0.6	1.5 ± 0.3	1.3 ± 0.2
Spleen	0.8 ± 0.4	0.8 ± 0.2	0.6 ± 0.2	0.7 ± 0.3
Stomach	0.5 ± 0.4	0.3 ± 0.1	0.3 ± 0.3	0.4 ± 0.1
Large Intestine	6.2 ± 3.2	8.5 ± 1.3	0.9 ± 0.4	1.0 ± 0.2
Feces	15.5 ± 2.4	13.5 ± 1.6	0.5 ± 0.6	0.6 ± 0.3
Small Intestine	1.2 ± 0.8	0.8 ± 0.1	0.5 ± 0.1	0.6 ± 0.1
Kidney	2.0 ± 0.6	1.8 ± 0.3	1.4 ± 0.2	1.2 ± 0.3
Muscle	0.4 ± 0.0	0.4 ± 0.1	0.3 ± 0.2	0.2 ± 0.1
Bone	0.4 ± 0.1	0.5 ± 0.4	0.5 ± 0.3	0.4 ± 0.1
Skin	0.5 ± 0.1	1.0 ± 0.2	0.8 ± 0.4	0.8 ± 0.3

Supplemental Table 6. Biodistribution data (%ID/g ± SD) of pre-targeting experiment with A33-TCO and ^{64}Cu-Tz-Bn-NOTA versus time in mice bearing subcutaneous SW1222 xenografts (n = 4 for each time point). Mice were administered A33-TCO (300 μg in 200 μL 0.9% sterile saline) via intravenous tail vein injection. After 24 h, the same mice were administered ^{64}Cu-Tz-Bn-NOTA (0.55 – 0.75 MBq [15-20 μCi] in 200 μL 0.9% sterile saline) via intravenous tail vein injection (t = 0). Stomach, small intestine, and large intestine contents were removed before weighing and activity measurement.

	1 h	4 h	12 h	24 h
Tumor/Blood	0.5 ± 0.2	0.6 ± 0.1	0.9 ± 0.2	1.1 ± 0.5
Tumor/Tumor	1.0 ± 0.4	1.0 ± 0.2	1.0 ± 0.1	1.0 ± 0.6
Tumor/Heart	1.5 ± 0.6	1.8 ± 0.5	2.1 ± 0.5	2.5 ± 1.3
Tumor/Lung	1.1 ± 0.4	1.7 ± 0.4	2.2 ± 0.2	2.0 ± 1.2
Tumor/Liver	1.2 ± 0.6	1.7 ± 0.5	2.4 ± 0.5	2.8 ± 1.3
Tumor/Spleen	3.7 ± 2.0	4.5 ± 1.2	5.8 ± 2.0	5.1 ± 3.0
Tumor/Stomach	5.6 ± 4.3	12.1 ± 4.4	10.7 ± 8.5	8.6 ± 4.0
Tumor/LI	0.5 ± 0.3	0.4 ± 0.1	3.8 ± 1.5	3.6 ± 1.7
Tumor/Feces	0.2 ± 0.1	0.3 ± 0.0	7.0 ± 7.7	6.6 ± 4.6
Tumor/SI	2.5 ± 1.8	4.9 ± 0.8	6.7 ± 1.9	6.3 ± 3.2
Tumor/Kidney	1.5 ± 0.7	2 ± 0.4	2.6 ± 0.5	3.1 ± 1.6
Tumor/Muscle	7.6 ± 2.4	9.9 ± 4.0	10.7 ± 5.3	15.2 ± 9.7
Tumor/Bone	7.5 ± 3.0	7 ± 4.9	7.2 ± 4.0	9.6 ± 4.9
Tumor/Skin	6.0 ± 2.4	3.9 ± 1.0	4.4 ± 2.0	4.6 ± 2.6

Supplemental Table 7. Tumor to tissue activity ratios from biodistribution data of pre-targeting with A33-TCO and ^{64}Cu-Tz-Bn-NOTA versus time (see Supplemental Table 6) in mice bearing subcutaneous SW1222 xenografts (n = 4 for each time point).

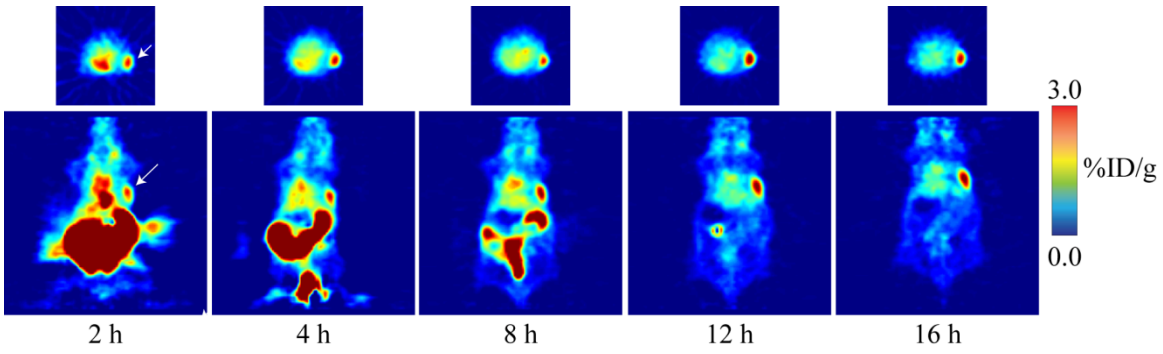

Supplemental Figure 10. Pre-targeting PET imaging. Mice bearing subcutaneous SW1222 (right shoulder, white arrow) xenografts (100-150 mm^3, 9-12 days post-inoculation) were administered A33-TCO (100 μg in 200 μL 0.9% sterile saline) via intravenous tail vein injection. After 12 h, the same mice were administered ^{64}Cu-Tz-Bn-NOTA (10.2 – 12.0 MBq, 275-325 μCi, ~1 μg) in 200 μL 0.9% sterile saline via intravenous tail vein injection. The transverse (top) and coronal (bottom) planar images intersect the center of the tumors.

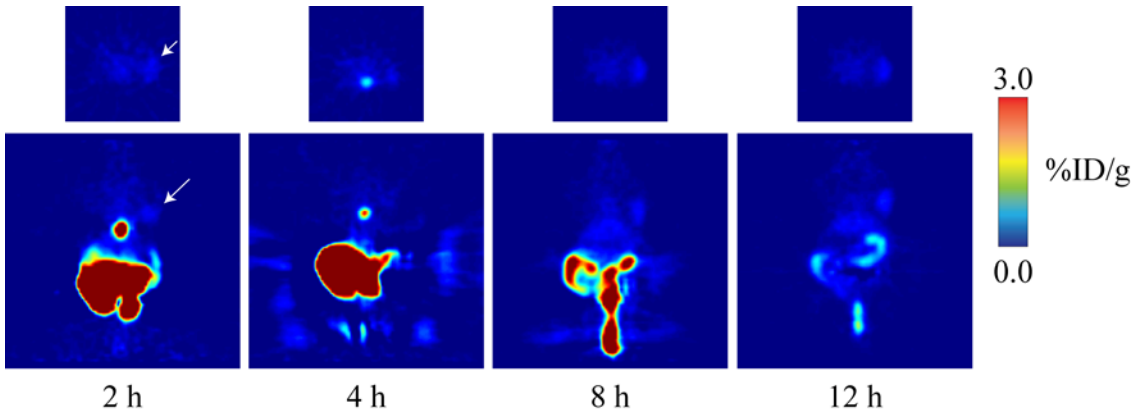

Supplemental Figure 11. Pre-targeted PET imaging experiment with low specific activity ^{64}Cu-Tz-Bn-NOTA. Mice bearing subcutaneous SW1222 (right shoulder, white arrow) xenografts (100-150 mm^3, 9-12 days post-inoculation) were administered A33-TCO (100 μg in 200 μL 0.9% sterile saline) via intravenous tail vein injection. After 24 h, the same mice were administered ^{64}Cu-Tz-Bn-NOTA (10.2 – 12.0 MBq, 275-325 μCi, ~1 μg) mixed with cold Tz-Bn-NOTA (50 μg) in 200 μL 0.9% sterile saline via intravenous tail vein injection. The transverse (top) and coronal (bottom) planar images intersect the center of the tumors.

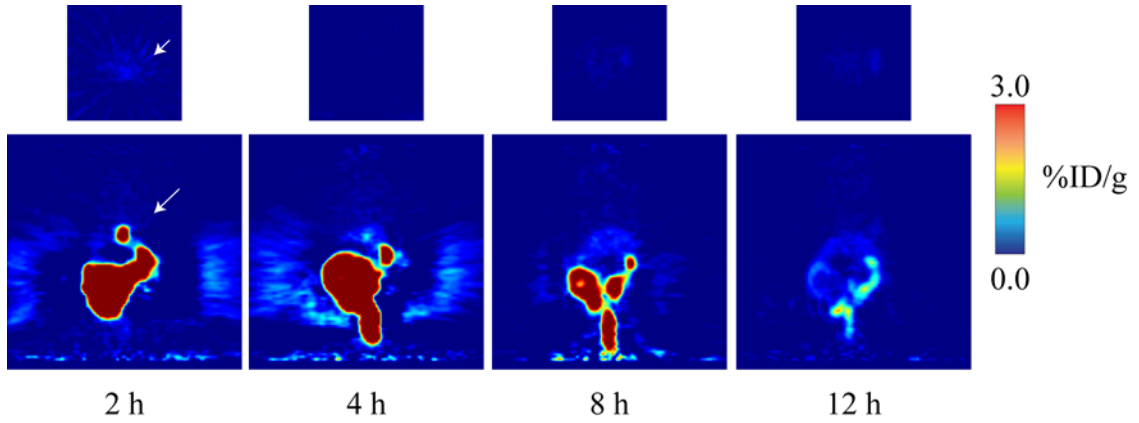

Supplemental Figure 12. ^{64}Cu-Tz-Bn-NOTA-only control experiment for pre-targeted PET imaging. Mice bearing subcutaneous SW1222 (right shoulder, white arrow) xenografts (100-150 mm^3, 9-12 days post-inoculation) were administered ^{64}Cu-Tz-Bn-NOTA (10.2 – 12.0 MBq, 275-325 μCi, ~1 μg) 200 μL 0.9% sterile saline via intravenous tail vein injection. The transverse (top) and coronal (bottom) planar images intersect the center of the tumors.

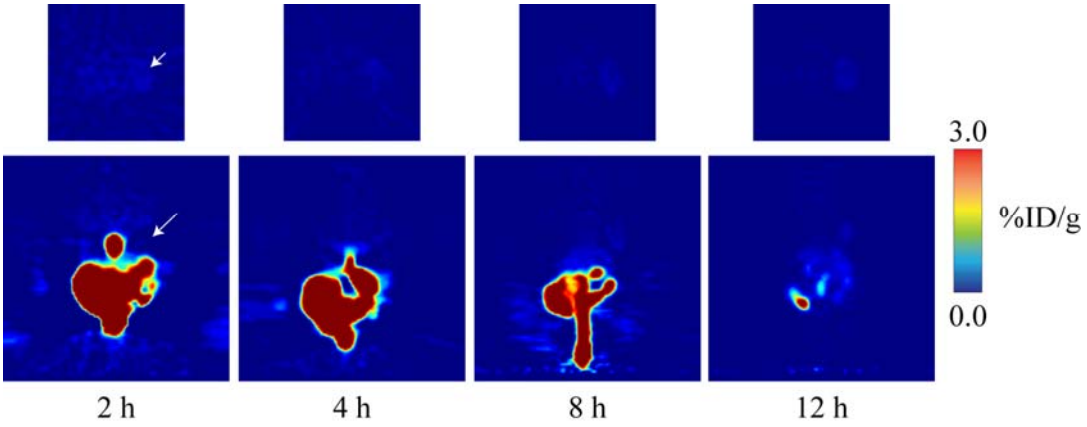

Supplemental Figure 13. Control experiment for pre-targeted PET imaging. Mice bearing subcutaneous SW1222 (right shoulder, white arrow) xenografts (100-150 mm^3, 9-12 days post-inoculation) were administered A33 (note: not A33-TCO) (100 μg in 200 μL 0.9% sterile saline) via intravenous tail vein injection. After 24 h, the same mice were administered ^{64}Cu-Tz-Bn-NOTA (10.2 – 12.0 MBq, 275-325 μCi, ~1 μg) mixed with cold Tz-Bn-NOTA (25 μg) in 200 μL 0.9% sterile saline via intravenous tail vein injection. The transverse (top) and coronal (bottom) planar images intersect the center of the tumors.

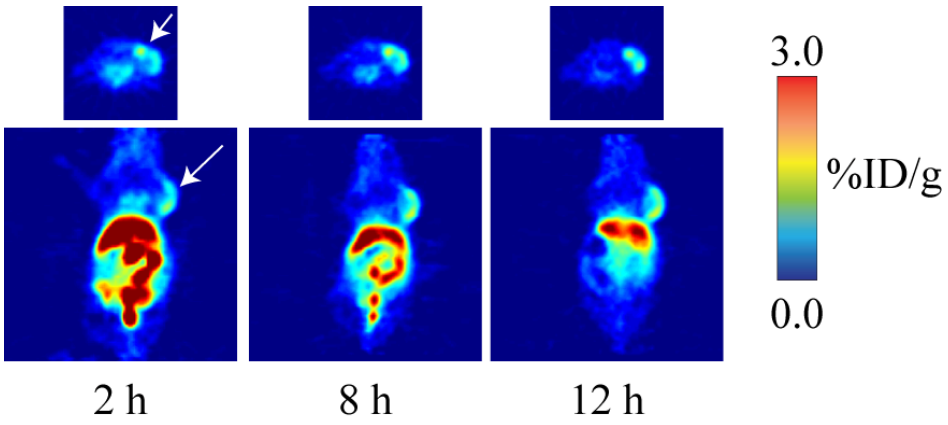

Supplemental Figure 14. Control experiment for pre-targeted PET imaging. Mice bearing subcutaneous SW1222 (right shoulder, white arrow) xenografts (100-150 mm^3, 9-12 days post-inoculation) were administered IgG-TCO (Sigma, isolated from mouse serum, 100 μg in 200 μL 0.9% sterile saline) via intravenous tail vein injection. After 24 h, the same mice were administered ^{64}Cu-Tz-Bn-NOTA (10.2 – 12.0 MBq, 275-325 μCi, ~1 μg) mixed with cold Tz-Bn-NOTA (25 μg) in 200 μL 0.9% sterile saline via intravenous tail vein injection. The transverse (top) and coronal (bottom) planar images intersect the center of the tumors.

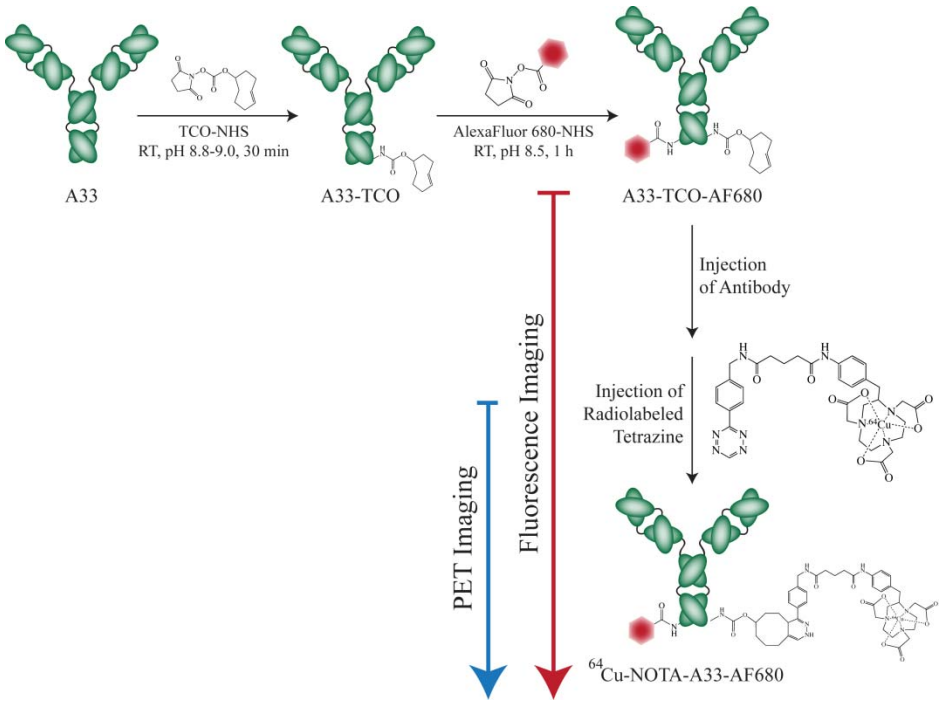

Supplemental Figure 15. Schematic of the fluorescence and PET multimodality imaging experiment. Mice bearing 9-12 day old SW1222 xenografts on the right shoulder were injected via tail vein with 100 μg A33-TCO-AF680. Fluorescence images were acquired 24 h post-injection. The animals were then immediately injected via tail vein with ^{64}Cu-Tz-Bn-NOTA (10.2 – 12.0 MBq, 275-325 μCi, ~1 μg) in 200 μL 0.9% sterile saline. At 12 h post-injection of the radiotracer (36 h post-injection of the antibody), PET and fluorescence images were acquired. This strategy allows for the tracking of both moieties in the antibody pre-targeting scheme.

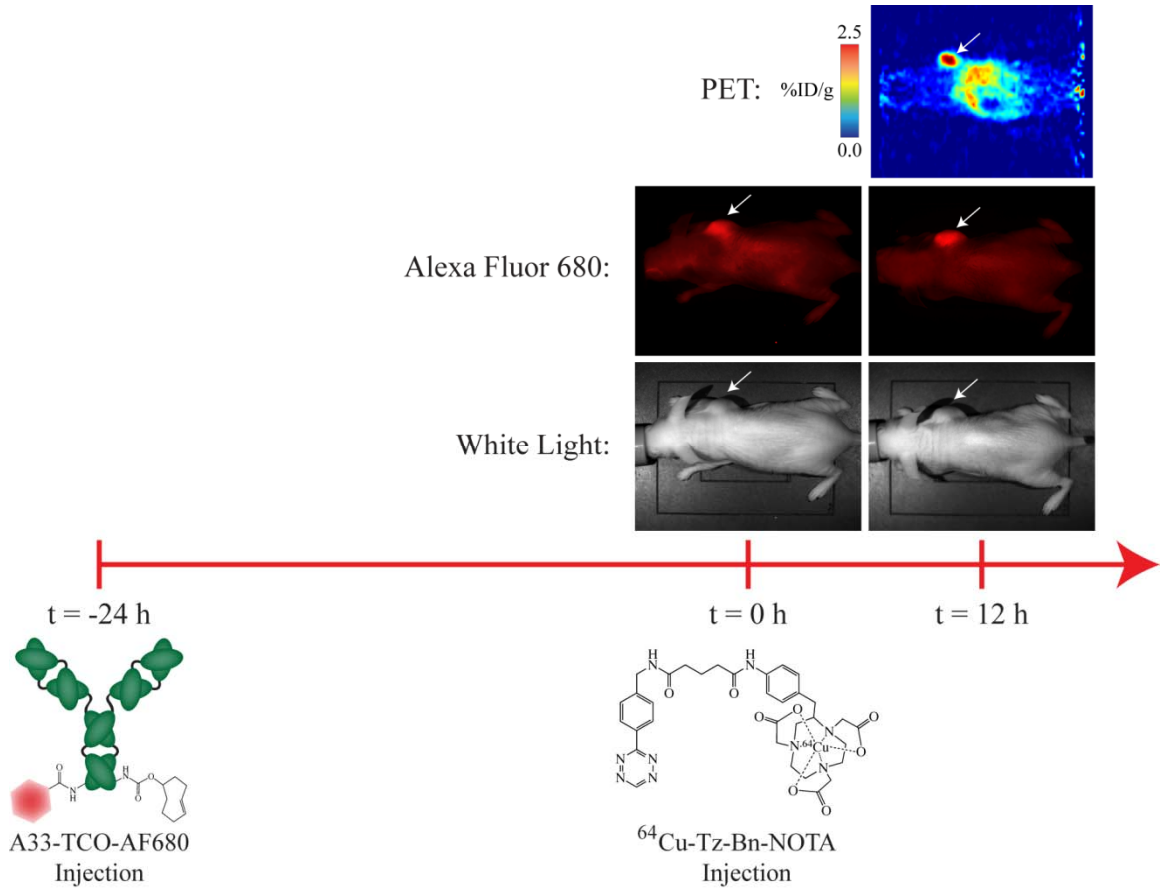

Supplemental Figure 16. *In vivo* fluorescence and PET multimodality imaging experiment. Mice bearing 9-12 day old SW1222 xenografts on the right shoulder were injected via tail vein with 100 μg A33-TCO-AF680. Fluorescence images were acquired 24 h post-injection. The animals were then immediately injected via tail vein with ^{64}Cu-Tz-Bn-NOTA (10.2 – 12.0 MBq, 275-325 μCi, ~1 μg) in 200 μL 0.9% sterile saline. At 12 h post-injection of the radiotracer (36 h post-injection of the antibody), PET and fluorescence images were acquired. The slightly increased background uptake in the PET image may result from a reduction in the immunoreactivity of the heavily modified A33-AF680-TCO.

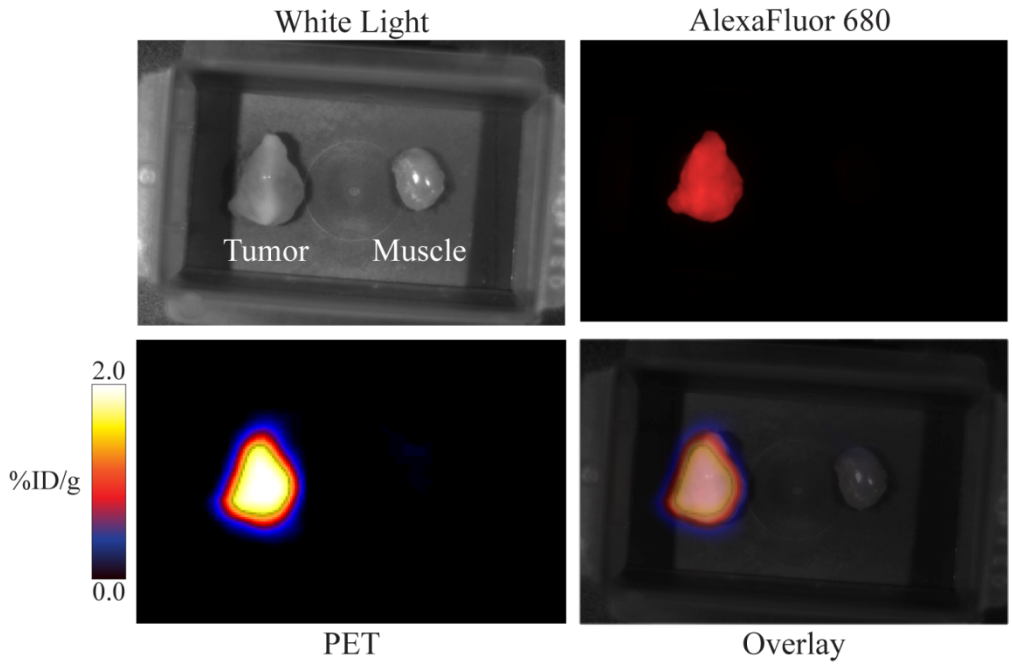

Supplemental Figure 17. *Ex vivo* fluorescence and PET imaging. Following the *in vivo* multimodality imaging experiment described above in Supplemental Figure 16, the mice were sacrificed, and tumor and muscle were removed for white light (top left), fluorescence (top right), and PET (bottom left) imaging. The bottom right image is a representative overlay of all three images.

	4 h	12 h	24 h	48 h
Blood	23.0 ± 3.6	21.3 ± 3.7	11.5 ± 1.6	1.4 ± 0.6
Tumor	18.2 ± 3.0	33.1 ± 7.0	33.6 ± 2.0	35.0 ± 3.8
Heart	10.2 ± 1.9	10.3 ± 1.3	3.0 ± 0.4	1.3 ± 0.6
Lung	13.9 ± 2.2	10.5 ± 2.0	3.7 ± 1.0	1.7 ± 1.0
Liver	16.7 ± 2.1	10.1 ± 1.6	10.6 ± 3.9	3.5 ± 1.5
Spleen	14 ± 5.0	7.0 ± 3.2	8.0 ± 4.7	1.8 ± 0.4
Stomach	2.7 ± 1.0	1.3 ± 0.5	2.5 ± 0.6	0.6 ± 0.2
Large Intestine	6.4 ± 0.7	6.3 ± 0.5	7.9 ± 1.2	3.1 ± 1.4
Feces	5.8 ± 2.3	2.9 ± 1.8	4.9 ± 1.3	3.0 ± 0.6
Small Intestine	8.9 ± 3.3	3.4 ± 0.6	5.0 ± 1.3	1.4 ± 0.3
Kidney	8.7 ± 2.7	6.5 ± 1.1	3.6 ± 0.8	1.8 ± 0.5
Muscle	1.1 ± 0.2	1.1 ± 1.0	1.0 ± 0.2	0.7 ± 0.3
Bone	5.8 ± 4.1	2.5 ± 0.7	5.0 ± 2.2	1.5 ± 0.5
Skin	6.0 ± 1.4	7.3 ± 1.7	4.0 ± 2.3	1.8 ± 0.8

Supplemental Table 8. Biodistribution data (%ID/g ± SD) of ^{64}Cu-NOTA-A33 versus time in mice bearing subcutaneous SW1222 xenografts (n = 4 for each time point). Tumor-bearing mice were randomized before the study and were warmed gently with a heat lamp for 5 min before administration of ^{64}Cu-NOTA-A33 (0.55 – 0.75 MBq [15-20 μCi] in 200 μL 0.9% sterile saline, 4-6 μg mAb) via intravenous tail vein injection (t = 0). Animals (n = 4 per group) were euthanized by CO_2(g) asphyxiation at 4, 12, 24, and 48 h. Stomach, small intestine, and large intestine contents were removed before weighing and activity measurement.

	4 h	12 h	24 h	48 h
Tumor/Blood	0.8 ± 0.2	1.6 ± 0.4	2.9 ± 0.4	24.5 ± 11.6
Tumor/Tumor	1.0 ± 0.2	1.0 ± 0.3	1.0 ± 0.1	1.0 ± 0.2
Tumor/Heart	1.8 ± 0.4	3.2 ± 0.8	11.0 ± 1.5	28.0 ± 14.7
Tumor/Lung	1.3 ± 0.3	3.1 ± 0.9	9.1 ± 2.6	20.8 ± 13.1
Tumor/Liver	1.1 ± 0.2	3.3 ± 0.9	3.2 ± 1.2	10.0 ± 4.5
Tumor/Spleen	1.3 ± 0.5	4.7 ± 2.3	4.2 ± 2.5	19.8 ± 5.4
Tumor/Stomach	6.8 ± 2.8	24.9 ± 10.7	13.2 ± 3.4	59.4 ± 19.7
Tumor/LI	2.8 ± 0.6	5.3 ± 1.2	4.2 ± 0.7	11.2 ± 5.3
Tumor/Feces	3.2 ± 1.3	11.3 ± 7.4	6.9 ± 1.9	11.7 ± 2.5
Tumor/SI	2.1 ± 0.8	9.7 ± 2.7	6.7 ± 1.8	25.0 ± 6.8
Tumor/Kidney	2.1 ± 0.7	5.0 ± 1.4	9.3 ± 2.1	20.0 ± 6.3
Tumor/Muscle	16.9 ± 3.8	29.5 ± 25.9	33.8 ± 6.7	52.2 ± 14.7
Tumor/Bone	3.2 ± 2.3	13 ± 4.5	6.7 ± 3.0	23.4 ± 8.3
Tumor/Skin	3.1 ± 0.9	4.5 ± 1.4	8.4 ± 5.0	19.6 ± 9.1

Supplemental Table 9. Tumor to tissue activity ratios from biodistribution data of ^{64}Cu-NOTA-A33 versus time (see Supplemental Table 8) in mice bearing subcutaneous SW1222 xenografts (n = 4 for each time point).

	4 h	12 h	24 h	48 h
Blood	35.6 ± 5.6	24.8 ± 2.4	11.1 ± 3.3	7.6 ± 2.2
Tumor	22.0 ± 2.1	30.7 ± 4.0	33.5 ± 3.8	35.5 ± 3.7
Heart	13.6 ± 2.3	10.2 ± 1.8	7.1 ± 1.4	3.2 ± 0.8
Lung	15.1 ± 2.7	13.9 ± 2.7	9.6 ± 2.7	4.5 ± 1.0
Liver	16.3 ± 0.8	9.8 ± 1.9	11.3 ± 1.3	4.6 ± 0.6
Spleen	9.7 ± 1.1	6.0 ± 0.7	6.1 ± 0.9	2.8 ± 0.7
Stomach	0.8 ± 0.4	1.2 ± 0.5	0.9 ± 0.2	1.1 ± 0.3
Large Intestine	6.3 ± 1.1	4.4 ± 0.6	5.8 ± 0.9	3.5 ± 0.5
Feces	3.2 ± 1.9	1.0 ± 0.3	3.9 ± 2.1	2.5 ± 0.9
Small Intestine	4.7 ± 1.0	3.1 ± 0.5	2.8 ± 0.3	1.5 ± 0.3
Kidney	11.9 ± 1.4	8.0 ± 0.6	5.9 ± 0.8	3.4 ± 0.6
Muscle	1.1 ± 0.1	1.7 ± 0.8	1.5 ± 0.5	1.2 ± 0.8
Bone	4.6 ± 1.0	4.1 ± 1.0	3.5 ± 1.0	2.1 ± 0.6
Skin	4.1 ± 1.6	6.1 ± 2.1	6.0 ± 2.4	4.2 ± 0.5

Supplemental Table 10. Biodistribution data (%ID/g ± SD) of ^{64}Cu-NOTA-A33 versus time in mice bearing subcutaneous SW1222 xenografts (n = 4 for each time point). Tumor-bearing mice were randomized before the study and were warmed gently with a heat lamp for 5 min before administration of ^{64}Cu-NOTA-A33 (0.55 – 0.75 MBq [15-20 μCi] in 200 μL 0.9% sterile saline, 100 μg mAb) via intravenous tail vein injection (t = 0). Animals (n = 4 per group) were euthanized by CO_2(g) asphyxiation at 4, 12, 24, and 48 h. Stomach, small intestine, and large intestine contents were removed before weighing and activity measurement.

	4 h	12 h	24 h	48 h
Tumor/Blood	0.6 ± 0.1	1.2 ± 0.2	3.0 ± 1.4	4.7 ± 1.4
Tumor/Tumor	1.0 ± 0.1	1.0 ± 0.2	1.0 ± 0.2	1.0 ± 0.1
Tumor/Heart	1.6 ± 0.3	3.0 ± 0.7	4.7 ± 1.1	11.0 ± 2.9
Tumor/Lung	1.5 ± 0.3	2.2 ± 0.5	3.5 ± 1.1	8.0 ± 1.9
Tumor/Liver	1.3 ± 0.1	3.1 ± 0.7	3.0 ± 0.5	7.7 ± 1.3
Tumor/Spleen	2.3 ± 0.3	5.1 ± 0.9	5.5 ± 1.0	12.7 ± 3.5
Tumor/Stomach	26.5 ± 11.7	26.2 ± 11	38.7 ± 9.1	31.1 ± 8.1
Tumor/LI	3.5 ± 0.7	6.9 ± 1.3	5.8 ± 1.2	10.1 ± 1.7
Tumor/Feces	6.9 ± 4.2	31.5 ± 9.7	8.6 ± 4.8	14.4 ± 5.6
Tumor/SI	4.7 ± 1.1	9.9 ± 2.0	11.9 ± 1.9	24.5 ± 6.1
Tumor/Kidney	1.9 ± 0.3	3.8 ± 0.6	5.7 ± 1.0	10.3 ± 2.2
Tumor/Muscle	20.2 ± 3.3	18.1 ± 8.4	21.6 ± 7.3	29.3 ± 18.8
Tumor/Bone	4.8 ± 1.1	7.5 ± 2.0	9.7 ± 3.1	16.9 ± 5.0
Tumor/Skin	5.4 ± 2.2	5.0 ± 1.8	5.5 ± 2.3	8.4 ± 1.4

Supplemental Table 11. Tumor to tissue activity ratios from biodistribution data of ^{64}Cu-NOTA-A33 versus time (see Supplemental Table 10) in mice bearing subcutaneous SW1222 xenografts (n = 4 for each time point).

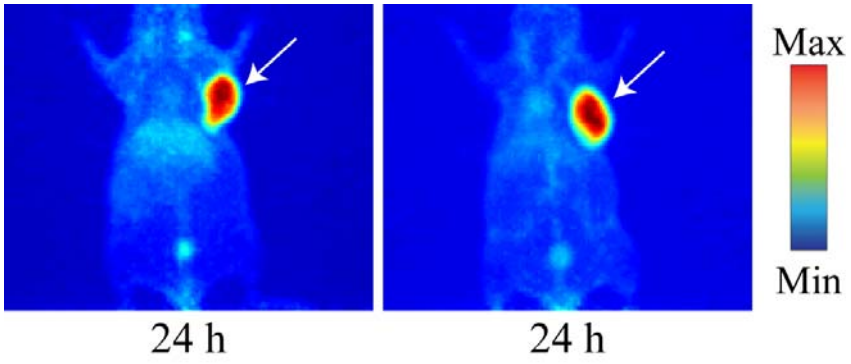

Supplemental Figure 18. Maximum intensity projection (MIP) PET images (two different mice) of ^{64}Cu-NOTA-A33 (10.2 – 12.0 MBq [275-325 μCi] in 200 μL 0.9% sterile saline via tail vein) in mice bearing a SW1222 xenograft (right shoulder, white arrow) at 24 h post-injection.

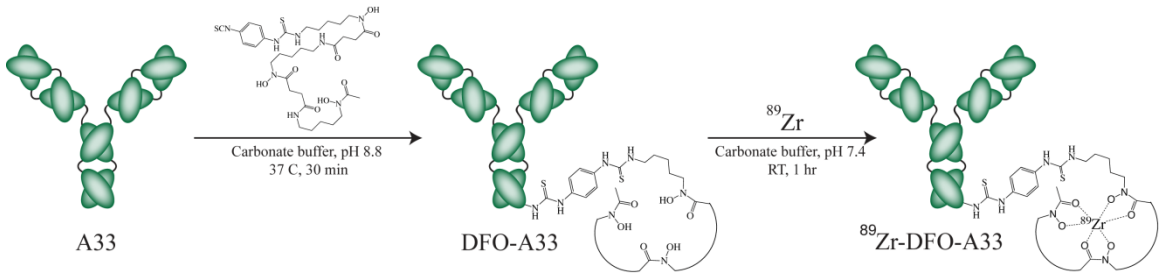

Supplemental Figure 19. Schematic of conjugation of A33 with DFO and subsequent labeling with ^{89}Zr.

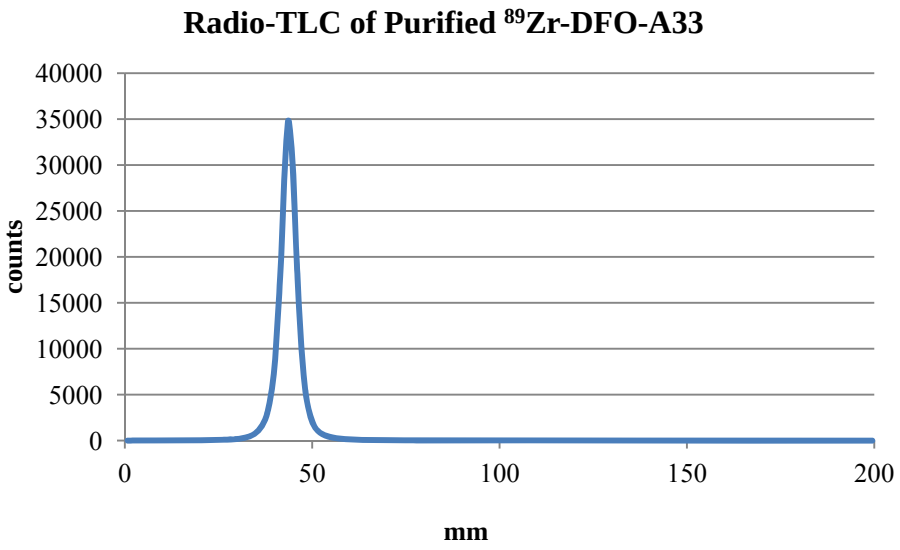

Supplemental Figure 20. Radio-TLC of purified ^{89}Zr-DFO-A33.

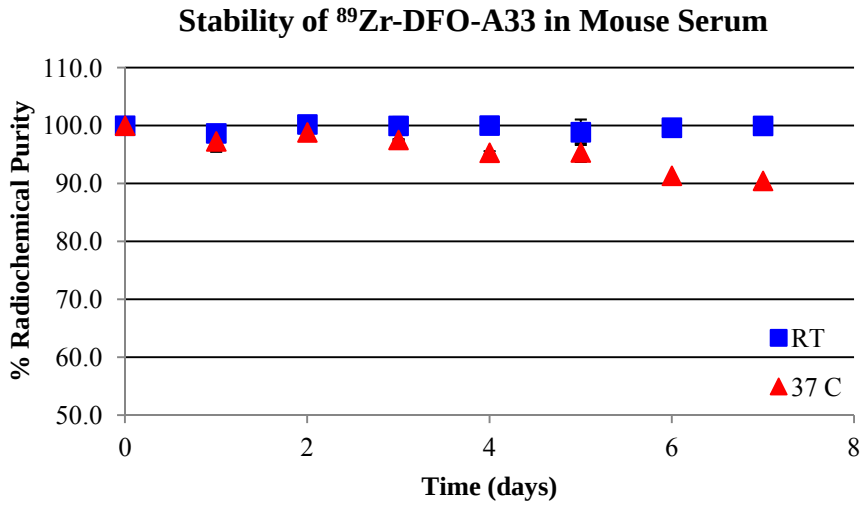

Supplemental Figure 21. Stability of ^{89}Zr-DFO-A33 to demetalation in mouse serum over the course of 7 days at room temperature (blue) or 37 ºC (red). Error bars mark standard deviation from the mean (n = 3).

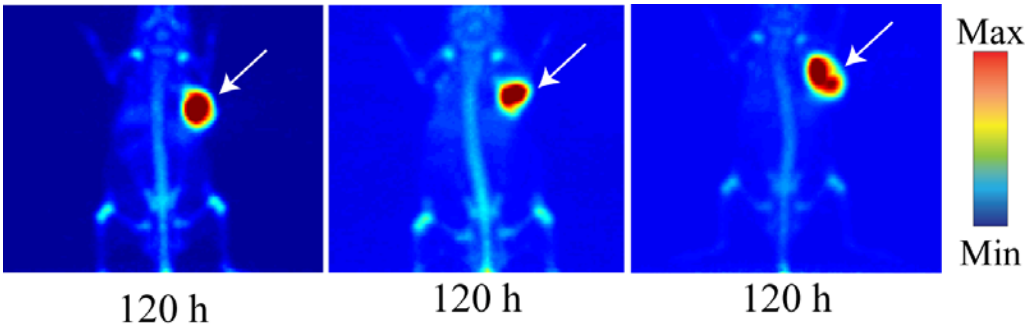

Supplemental Figure 22. Maximum intensity projection (MIP) PET images of ^{89}Zr-DFO-A33 (10.2 – 12.0 MBq [275-325 μCi] in 200 μL 0.9% sterile saline via tail vein) in mice bearing a SW1222 xenograft (right shoulder, white arrow) between at 120 h post-injection (three different mice). Note the activity in the bone.

	4 h	24 h	48 h	72 h	96 h	120 h
Blood	58.5 ± 8.5	18.3 ± 4.0	6.5 ± 2.6	3.9 ± 3.4	3.7 ± 3.7	2.3 ± 1.7
Tumor	31 ± 3.6	43.3 ± 9.0	44.7 ± 10.5	40.5 ± 4.4	27.6 ± 4.1	30.0 ± 5.1
Heart	24.0 ± 6.5	11.7 ± 1.8	4.0 ± 0.8	3.3 ± 1.4	2.7 ± 1.6	2.3 ± 1.0
Lung	40.1 ± 3.3	14.8 ± 1.6	6.7 ± 2.1	3.9 ± 2.6	3.1 ± 2.5	1.1 ± 0.4
Liver	24.0 ± 2.9	14.4 ± 6.2	7.3 ± 1.6	5.7 ± 3.6	4.5 ± 2.2	1.6 ± 1
Spleen	18.7 ± 4.2	13.4 ± 7.8	8.9 ± 1.4	5.5 ± 2.0	5.4 ± 0.7	2.2 ± 1.2
Stomach	2.8 ± 0.5	3.8 ± 0.9	1.7 ± 0.3	1.0 ± 0.1	1.0 ± 0.7	2.0 ± 2.5
L. Intestine	2.7 ± 0.6	3.4 ± 1.5	1.4 ± 0.3	0.5 ± 0.2	0.4 ± 0.3	0.5 ± 0.3
S. Intestine	4.4 ± 0.8	7.6 ± 4.3	2.2 ± 0.6	2.6 ± 0.6	1.1 ± 0.6	2.1 ± 2.5
Kidney	18.0 ± 1.3	9.8 ± 0.7	5.3 ± 0.5	3.3 ± 1	2.5 ± 2.0	2.8 ± 2.0
Muscle	2.8 ± 0.2	3.4 ± 0.5	1.9 ± 0.5	0.7 ± 0	0.7 ± 0.1	1.1 ± 1.0
Bone	11.7 ± 3	12.3 ± 4.5	12.0 ± 1.4	12.9 ± 5.7	4.8 ± 0.9	6.9 ± 2.0
Skin	5.9 ± 1.2	9.1 ± 0.7	6.2 ± 1	2.1 ± 0.3	2.3 ± 1.1	1.9 ± 0.5

Supplemental Table 12. Biodistribution data (%ID/g ± SD) of ^{89}Zr-DFO-A33 versus time in mice bearing subcutaneous SW1222 xenografts (n = 4 for each time point). Tumor-bearing mice were randomized before the study and were warmed gently with a heat lamp for 5 min before administration of ^{89}Zr-DFO-A33 (0.55 – 0.75 MBq [15-20 μCi] in 200 μL 0.9% sterile saline, 4-6 μg) via intravenous tail vein injection (t = 0). Animals (n = 4 per group) were euthanized by CO_2(g) asphyxiation at 4, 24, 48, 72, 96, and 120 h. Stomach, small intestine, and large intestine contents were removed before weighing and activity measurement.

	4 h	24 h	48 h	72 h	96 h	120 h
Tumor/Blood	0.5 ± 0.1	2.4 ± 0.7	6.9 ± 3.2	10.3 ± 9.1	7.4 ± 7.5	13.0 ± 9.7
Tumor/Tumor	1.0 ± 0.2	1.0 ± 0.3	1.0 ± 0.3	1.0 ± 0.2	1.0 ± 0.2	1.0 ± 0.2
Tumor/Heart	1.3 ± 0.4	3.7 ± 1.0	11.2 ± 3.4	12.4 ± 5.3	10.4 ± 6.3	13 ± 6.3
Tumor/Lung	0.8 ± 0.1	2.9 ± 0.7	6.7 ± 2.6	10.3 ± 7.0	8.8 ± 7.2	28.3 ± 12.6
Tumor/Liver	1.3 ± 0.2	3.0 ± 1.4	6.1 ± 1.9	7.2 ± 4.7	6.1 ± 3.1	19.3 ± 12.4
Tumor/Spleen	1.7 ± 0.4	3.2 ± 2.0	5.0 ± 1.4	7.4 ± 2.9	5.1 ± 1.0	13.8 ± 7.9
Tumor/Stomach	11 ± 2.3	11.3 ± 3.6	26.6 ± 7.8	41.2 ± 6.9	28 ± 19.5	14.9 ± 18.4
Tumor/LI	11.5 ± 2.9	12.9 ± 6.2	31.7 ± 10	77.1 ± 30.1	62.3 ± 36.4	63.9 ± 37
Tumor/SI	7.0 ± 1.5	5.7 ± 3.4	20.1 ± 7.1	15.6 ± 4.1	25.2 ± 13.9	14.2 ± 16.8
Tumor/Kidney	1.7 ± 0.2	4.4 ± 1.0	8.4 ± 2.1	12.2 ± 3.8	10.9 ± 8.7	10.8 ± 8.1
Tumor/Muscle	10.9 ± 1.6	12.7 ± 3.3	23.2 ± 7.7	57.7 ± 7.0	37.1 ± 8.6	26.3 ± 23.5
Tumor/Bone	2.6 ± 0.8	3.5 ± 1.5	3.7 ± 1.0	3.1 ± 1.4	5.7 ± 1.4	4.3 ± 1.5
Tumor/Skin	5.2 ± 1.2	4.7 ± 1	7.2 ± 2.0	19.4 ± 3.2	12.1 ± 6.3	15.7 ± 5.1

Supplemental Table 13. Tumor to tissue activity ratios from biodistribution data of ^{89}Zr-DFO-A33 versus time (see Supplemental Table 12) in mice bearing subcutaneous SW1222 xenografts (n = 4 for each time point).

REFERENCES

1. Anderson CJ, Connett JM, Schwarz SW, et al. Copper-64-labeled antibodies for PET imaging. J Nucl Med. 1992;33:1685-91.
2. Holland JP, Caldas-Lopes E, Divilov V, et al. Measuring the pharmacodynamic effects of a novel Hsp90 inhibitor on HER2/neu expression in mice using Zr-89-DFO-trastuzumab. PLoS One. 2010;5:e8859.
3. Lindmo T, Boven E, Cuttitta F, Fedorko J, Bunn PA, Jr. Determination of the immunoreactive fraction of radiolabeled monoclonal antibodies by linear extrapolation to binding at infinite antigen excess. J Immunol Methods. 1984;72:77-89.
4. Lindmo T, Bunn PA, Jr. Determination of the true immunoreactive fraction of monoclonal antibodies after radiolabeling. Methods Enzymol. 1986;121:678-91.
5. Kim JS, Lee JS, Im KC, et al. Performance measurement of the microPET Focus 120 scanner. J Nucl Med. 2007;48:1527-35.
6. Carlin S, Khan N, Ku T, Longo VA, Larson SM, Smith-Jones PM. Molecular targeting of carbonic anhydrase IX in mice with hypoxic HT29 colorectal tumor xenografts. PLoS ONE. 2010;5:e10857.
7. Carlin S, Pugachev A, Sun X, et al. In vivo characterization of a reporter gene system for imaging hypoxia-induced gene expression. Nucl Med Biol. 2009;36:821-31.
8. Cristy M, Eckerman K. Specific absorbed fractions of energy at various ages from internal photon sources (I-VII). Springfield, VA: National Technical Information Service, Department of Commerce;1987.
9. Stabin MG, Sarks RB, Crowe E. OLINDA/EXM: the second-generation personal computer software for internal dose assessment in nuclear medicine. J Nucl Med. 2005;45:1023-7.